

Optimization of Process Parameters in the Hole Sinking Electrical Discharge Micromachining of Ti-6Al-4V Thin Sheet

Rajesh Kumar Porwal¹ * and Vinod Yadav²

¹ME, Department, KCC Institute of Technology & Management, Gr. Noida, Uttar Pradesh - 201306, India

²ME, Department, Motilal Nehru National Institute of Technology, Allahabad, Uttar Pradesh - 211004, India

Email: porwal.rajesh@gmail.com

Abstract – The paper describes the multi-objective optimization of hole sinking electrical discharge micromachining (HS-EDMM) process considering material removal rate (MRR), tool wear rate (TWR), and hole taper (T_a) as objectives simultaneously. The micromachining parameters considered in the present work are gap voltage and capacitance of capacitor. Eighteen set of experiments are conducted as per L_{18} orthogonal array and these experimental results are used for further optimization. Optimal combination of process parameters is determined using grey relational analysis that employs grey relational grade as performance indexes. The principal component analysis is applied to evaluate the weighting values corresponding to each performance characteristics so that their relative importance can be properly and objectively described. Optimal combination of the process parameters for the multi-performance characteristics of the hole sinking electrical discharge machining has been found as; gap voltage 140V and 100 pF capacitance of capacitor.

Keywords: Hole sinking electrical discharge micromachining, HS-EDMM, Optimization, GRA, grey relational analysis, PCA, principal component analysis.

I. INTRODUCTION

In recent years, there is an increasing trend towards miniaturization of various engineering components. In view of this, micro machining techniques have become important in the fabrication of micro components based on the different mechanism of material removal. These miniaturized components/ products having multi functional distinctiveness are largely employed in electronics, optics, automobile, biotechnology, and aeronautical industries. Based on the mechanism of material removal rate, micro machining are classified into various processes like micro electro discharge machining (μ -EDM), micro ultrasonic machining (μ -USM), micro beam machining processes (μ -BMPs), micro jet

machining processes (μ -JMPs), and micro chemical machining processes (μ -CMPs). Micro-EDM is one of the successful micro machining processes to create micro feature (order of few hundred of microns) in difficult to machine electrically conductive materials. The mechanism of material removal is similar to that of conventional EDM. The machine setup has a servo control system with the highest sensitivity and positional accuracy of $\pm 0.05\mu\text{m}$ along with the inter electrode gap of 1-5 μm . The power supply used in μ -EDM is relaxation or transistor type pulse generator with MHz of pulsating frequency. The efficiency of this process is high as the low specific energy of material removal at low discharge level [1]. There are many variations of μ -EDM depending on the configuration of tool and workpiece as well as the type of feature that can be created. Such variations can be classified as: Die Sinking-EDMM to create unsymmetrical features of small depth to diameter ratio, Hole Sinking-EDMM to create symmetrical features of relatively large depth to diameter ratio, Hole Drilling-EDMM, Pocket Milling-EDMM, Wire-EDMM, and Wire Micro-Electro Discharge Grinding (Wire-MEDG). In the present paper, the multiple responses MRR, TWR, and T_a are simultaneously optimized using L_{18} orthogonal array based experimentation and GRA couples with PCA during HS-EDMM process.

II. LITERATURE REVIEW

Higher accuracy and miniaturization have been always the goals for the development of μ -EDM machines. Wong *et. al* [2] developed a single-spark generator to study the erosion characteristics from the micro crater size due to micro-EDM. Their experimental results suggested that volume and size of the micro craters are found to be more consistent at lower-energy discharges than at higher-energy discharges. An optical sensor has been developed by Lin and Ho [3] to measure and control the dimension of the thin electrode during the tool fabrication process. They observe

that the rotating electrode shows the best performance in the high-aspect ratio tool-electrode fabrication and machining depth is inversely proportional to the feed rate. A 4-axis μ -EDM machine using DC servo motors was developed by Zhao *et. al* [4]. They used granite base to decrease the stray capacitance for lower discharge energy, also a 25 μ m diameter micro-hole with aspect ratio over 10 was drilled on this machine. A 3-axis local actuator module for μ -EDM was developed by Imai *et.al* [5]. This module had 200 Hz bandwidth and utilized the electromagnetic force for the holding and positioning of the electrode. A 60 μ m diameter micro-hole with aspect ratio over 16 was machined by this module. Takezawa *et. al* [6] have developed a micro-EDM machining center, which was able to carried out on-the-machine measurement of the work piece shape and small holes or two-dimensional micromachining. Han *et. al* [7] have developed a new transistor type isopulse generator and servo feed control to improve the machining characteristics of micro-EDM. It is observed that the transistor type isopulse generator is more useful in semi finishing than in finishing, whereas servo feed control is better in finishing as compare to semi finishing.

Sona *et. al* [8] investigated the influences of electrical pulse condition on the machining properties in micro-EDM, they found that the voltage and current are proportional to the material removal rate, while current is only proportional in the case of tool wear rate. Also shorter pulse on duration is profitable to make accurate machining with a higher removal rate and a lower tool wear rate. Uhlmann *et. al* [9] studies the process behavior of boron doped CVD-diamond and polycrystalline diamond in micro-EDM well as influences of electrode materials on tool electrode wear and surface formation processes. Johan *et. al* [10] studied the effect of different tool electrode materials (W, AgW, CuW) on workpiece material (WC) for material removal rate (MRR) and tool wear rate (TWR). It was observed that the AgW electrode produces smoother and defect-free nano surface among the three electrodes. Besides, a minimum amount of material migrates from the AgW electrode to the WC workpiece during the finishing micro-EDM. CuW electrode achieved highest MRR while W electrode have lowest tool wear among all electrodes.

Dhanik *et. al* [11] have proposed a comprehensive model of micro-EDM process for a RC-pulse discharge circuitry considering the active role of plasma throughout the discharge. It includes the modeling of the breakdown phase, various

phenomena in the pre breakdown period, such as current emission and bubble nucleation at micro-peaks, leading to breakdown by electron-impact ionization. The effects of variable mass expansion plasma on the energy transferred to respective electrodes were also modeled using fluid dynamic and heat transfer equations. Kumar and Yadava [12] developed a finite element-based thermal model of micro-EDM for the determination of temperature distribution in the zone of influence of single spark, crater shape and size as a result of the material removal. Their calculated crater radius was verified with experimental results, and the parametric results shows that heat flux and input energy are inversely proportional to energy partition value, and the crater depth decreases with respect to increase in spark radius. Das and Joshi [13] have developed an analytical model that takes into account plasma features, moving heat source characteristics, multi-spark phenomenon, and wire vibrational effects to predict the cathode erosion rate for a single and multi-spark in micro-WEDM process. Karpat and Ozel [14] introduces a procedure to formulate and solve optimization problems for multiple and conflicting objectives that may exist in finish hard turning processes using neural network modeling together with dynamic neighborhood particle swarm optimization technique.

This study uses the TM to achieve the experimental data, employs the GRA to find the optimal processing parameters combination, and applies the PCA to remove the relativity among the qualities.

III. EXPERIMENTAL PLANNING

Hole sinking electrical discharge micromachining (HS-EDMM) was performed on multi process micro electro discharge machine (Model DT-110, Mikrotool Pte, Singapore), having fixed level of capacitance, and adjustable range of voltage. Tungsten carbide rod of 500 μ m diameter was used as tool electrode. The micro HS-EDMM operation was performed on rectangular section cuboid shape workpiece specimens made of Ti-6Al-4V having mean thickness of 0.5mm, length 25 mm, and width 15 mm. The removal of debris was achieved by lateral flushing with dielectric (EDM oil). The depth of cut was kept constant 510 micron for all experiments. In the present research, analysis of the effect of different parameter settings on material removal rate, tool wear rate, and hole taper was carried out. After preliminary investigations, two input parameters were selected as: gap voltage and capacitance of capacitor. Selection of the range of process parameter settings was made after performing some

pilot experiments within the stable domain of the machining. The levels of parameters selected are shown in Table I. The amount of material removed from the workpiece and tool electrode were measured with the help of citizen make micro weighing balance having least count of 0.0001grams.

Material removal rate (MRR) and tool wear rate (TWR) are defined as volume of material removed or wear in unit time from workpiece and tool electrode respectively.

TABLE I THE MACHINING PARAMETERS AND THEIR LEVELS

Machining parameters	Units	Level					
		1	2	3	4	5	6
Voltage	V	90	100	110	120	130	140
Capacitance	nF	10	100	400			

Hence, based on their density the MRR and TWR are calculated as;

$$MRR = \frac{\text{Mass of workpiece material removed}}{\text{Density of workpiece material} \times \text{Time to make hole}}$$

$$TWR = \frac{\text{Mass of tool electrode material removed}}{\text{Density of tool electrode material} \times \text{Time to make hole}}$$

In order to find machined hole taper (T_a), the diameter of hole at entrance and exit is measured using optical measuring microscope (Model SDM-TR-MSU, Sipcon Instrument Industries, India) at 10 x magnifications (as shown in Figure 1) and T_a was calculated as:

$$T_a (rad) = \frac{(\text{hole entrance diameter}) - (\text{hole exit diameter})}{2 \times \text{Workpiece thickness}}$$

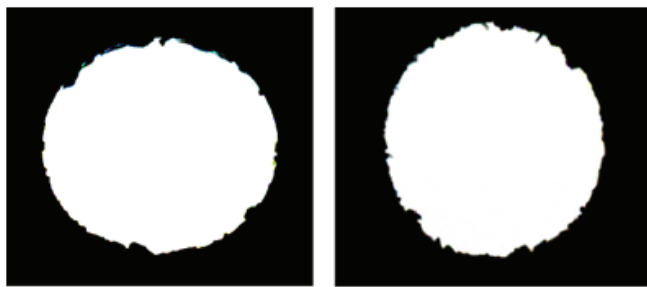


Fig. 1 Microscopic views of micro sinker holes at entry (a) and exit (b) with machining conditions 10V, 100 nF

Experiments were carried out using fractional factorial combinations of these factors and their different levels. During experiments the workpiece thickness was kept constant for all experimental run. Dielectric was also kept same for experimentation. As per Taguchi methodology an orthogonal array was selected based on the input parameters and their levels. Interaction effect was not taken into account. L_{18} orthogonal array was selected with one input parameters of three levels and other parameter of six levels. To achieve validity and accuracy, each test has been repeated three times. The responses considered were material removal rate, tool wear rate and hole taper of the micro through holes.

IV. OPTIMIZATION OF HS-MEDM USING GRA COUPLED WITH PCA

Selected combinations of input parameters were used as input parameter for optimization using grey relational analysis (GRA) coupled with principal component analysis (PCA). In GRA, all information represents in terms of black and white. Black represents having no information and white represents having all information [15]. Grey relational analysis can be used to represent the grade of correlation between two sequences so that the distance of two factors can be measured discretely. It helps to compensate the shortcomings of statistical regression by means of conducting less number of experiments, as experiments are ambiguous or experimental methods does not allow to do the exact number of experiments [16]. Grey relational analysis is an effective means of analyzing the relationship between sequences with less data and can analyze many factors that can overcome the disadvantages of statistical method [17]. The steps involved in performing grey relational analysis are to first preprocess the input data. It is required, as it relates to a group of sequences, this preprocessing generates the grey relational generation. Data preprocessing is a process of transferring the original sequence to a comparable sequence. For this purpose, the experimental results are normalized in the range between zero and one. In present study, normalization of MRR was done by using equation (2), as higher the better is required here, while normalization of TWR and overcut was done by using equation (1) because smaller the better is desired [18].

$$x_i^*(k) = \frac{x_i^0(k) - \min x_i^0(k)}{\max x_i^0(k) - \min x_i^0(k)} \tag{1}$$

$$x_i^*(k) = \frac{\max x_i^0(k) - x_i^0(k)}{\max x_i^0(k) - \min x_i^0(k)} \tag{2}$$

where, $x_i^*(k)$ is the value after the grey relational generation, $\max x_i^0(k)$ is the largest value of $x_i^0(k)$, $\min x_i^0(k)$ is the smallest value of $x_i^0(k)$. Table II lists all of the sequences following data pre-processing using equation (4) and equation (5). Also the deviation sequences Δ_{0i} , $\Delta_{max}(k)$, and $\Delta_{min}(k)$ for $i = 1$ to 18, $k = 1$ to 3 can be calculated using equations (4-6). These values of deviation sequences were used for further calculation of grey relational coefficients by using equation (3). The grey relational coefficient represents the relationship between the ideal and actual normalized experimental results. The grey relational coefficient can be expressed as follows [18]:

$$\xi_i(k) = \frac{\Delta_{min} + \zeta \cdot \Delta_{max}}{\Delta_{0i}(k) + \zeta \cdot \Delta_{max}} \quad (3)$$

Where $\Delta_{0i}(k)$ is the deviation sequence of the reference sequence $x_0^*(k)$ and the comparability sequence $x_i^*(k)$ namely

$$\Delta_{0i}(k) = \|x_0^*(k) - x_i^*(k)\| \quad (4)$$

$$\Delta_{max} = \max_{j \in i} \max_k \|x_0^*(k) - x_j^*(k)\| \quad (5)$$

$$\Delta_{min} = \min_{j \in i} \min_k \|x_0^*(k) - x_j^*(k)\| \quad (6)$$

ζ is the distinguishing coefficient, which is defined in the range $0 \leq \zeta \leq 1$, $\zeta = 0.5$ is generally used. After obtaining the grey relational coefficient, we normally take the average of the grey relational coefficient as the grey relational grade. The grey relational grade is defined as follows: [17].

$$\gamma_i = \frac{1}{n} \sum_{k=1}^n \xi_i(k) \quad (7)$$

However, since in present research the effect of each factor on the system is not exactly same. Eq. (7) can be modified as

$$\gamma_i = \frac{1}{n} \sum_{k=1}^n w_k \cdot \xi_i(k), \quad \sum_{k=1}^n w_k = 1 \quad (8)$$

where w_k represents the normalized weighting value of factor k. Given the same weights, Equation (7) and (8) are equal. In the grey relational analysis, the grey relational grade is used to show the relationship among the sequences. If the two sequences are identical, then the value of grey relational grade will be equal to 1. The grey relational grade also indicates the degree of influence that the comparability sequence could exert over the reference sequence. Therefore, if a particular comparability sequence is more important than

the other comparability sequences to the reference sequence, then the grey relational grade for that comparability sequence and reference sequence will be higher than other grey relational grades [19]. In this research the corresponding weighting values i.e. w_k are obtained from the principal component analysis. Principal component analysis (PCA) was developed by Hotelling [20].

This approach explains the structure of variance-covariance by the way of the linear combinations of each quality characteristic. The procedure is adapted to calculate the weight in the present research is as follows [21]; first we convert the calculated grey relational coefficient into matrix form as represented in equation (9), where m is the number of experiment and n is the number of the quality characteristic. In present study, x is the grey relational coefficient of each quality characteristic and m = 18, n = 3. The above matrix is used to find out the correlation coefficient. The array of correlation coefficient was calculated by using equation (10).

TABLE II THE SEQUENCES OF EACH PERFORMANCE CHARACTERISTIC AFTER DATA PRE-PROCESSING

Exp. No.	MRR	TWR	T _a
Reference sequence	1.0000	1.0000	1.0000
1	1.0000	0.0013	0.4819
2	0.8630	0.0493	0.0000
3	0.5832	0.2511	0.0939
4	0.9832	0.0000	0.5219
5	0.8589	0.0581	0.3353
6	0.5654	0.3497	0.0531
7	0.9791	0.0266	0.2583
8	0.8573	0.0810	1.0000
9	0.3676	0.3181	0.2788
10	0.9142	0.0785	0.6892
11	0.6272	0.1352	0.2788
12	0.1403	0.7406	0.6909
13	0.9303	0.0553	0.9715
14	0.6268	0.0793	0.0640
15	0.1198	0.7427	0.5749
16	0.6024	0.2520	0.0732
17	0.5341	0.0975	0.8318
18	0.0000	1.0000	0.7469

$$X = \begin{bmatrix} x_1(1) & x_1(2) & \dots & \dots & x_1(n) \\ x_2(1) & x_2(2) & \dots & \dots & x_2(n) \\ \vdots & \vdots & \dots & \dots & \vdots \\ \vdots & \vdots & \dots & \dots & \vdots \\ x_m(1) & x_m(2) & \dots & \dots & x_m(n) \end{bmatrix} \quad (9)$$

$$R_{jl} = \frac{Cov(x_i(j), x_i(l))}{\sigma_{(x_i)}(j) \times \sigma_{(x_i)}(l)}, \quad j = 1, 2, 3, 4, \dots, n; \quad (10)$$

$$l = 1, 2, 3, 4, \dots, n$$

here $Cov(x_i(j), x_i(l))$ is the covariance of sequences and $x_i(j)$, $\sigma_{(x_i)}(j)$ is the standard deviation of sequence $x_i(j)$ and $\sigma_{(x_i)}(l)$ is the standard deviation of sequence $x_i(l)$. After calculating correlation coefficient array, eigenvectors and eigenvalues were calculated by using equation (11). The procedure of getting eigenvectors and eigenvalues from correlation coefficient array is as follows

$$(R - \lambda_k I_m) V_{ik} = 0 \quad (11)$$

where λ_k eigenvalues,

$$\sum_{k=1}^n \lambda_k = n, k = 1, 2, 3, \dots, n$$

$$V_{ik} = [a_{k1} a_{k2} a_{k3} \dots a_{kn}]^T$$

is the eigenvectors corresponding to the eigenvalue λ_k . The eigenvectors and eigenvalues were further used to find principal components by using equation (12).

$$Y_{mk} = \sum_{i=1}^n x_m(i) V_{ik} \quad (12)$$

where Y_{m1} is called the first principal component, Y_{m2} is called the second principal component and so on. The principal components are aligned in descending order with respect to variance, and therefore the first principal component Y_{m1} accounts for most variance in the data, Table III.

TABLE III THE EIGENVALUES AND EXPLAINED VARIATION FOR PRINCIPAL COMPONENTS

Principal component	Eigenvalue	Explained variation (%)
First	1.9684	65.61
Second	0.973	32.43
Third	0.0586	1.95

TABLE IV THE EIGENVECTORS FOR PRINCIPAL COMPONENTS

Quality characteristic	Eigenvectors		
	First principal component	Second principal component	Third principal component
MRR	-0.7011	-0.053	0.7111
TWR	0.6819	0.2417	0.6904
T _a	0.2085	-0.9689	0.1333

TABLE V THE CONTRIBUTION OF EACH INDIVIDUAL QUALITY CHARACTERISTIC FOR THE PRINCIPAL COMPONENT

Quality characteristic	Contribution
MRR	0.49154
TWR	0.46499
T _a	0.04347

Next step is to find percentage contribution or explained variation of eigenvalues. The eigenvector corresponding to each eigenvalue is listed in Table IV. The eigenvectors corresponding to the largest eigenvalue were selected, and the square of the eigenvalue vectors corresponding to the first principal component represents the contribution of the respective performance characteristic to the principal component. The contribution of material removal rate, tool wear rate, and overcut is shown in Table V. These contributions are indicated as 0.4915, 0.4645, and 0.0434 for MRR, TWR, and T_a respectively. Moreover, the variance contribution for the first principal component characterizing the three performance characteristics is as high as 73.05%. Hence, for this study, the squares of its corresponding eigenvectors were selected as the weighting values of the related performance characteristic, and coefficients w_1 , w_2 and w_3 for equation (11) were thereby set as 0.4915, 0.4645, and 0.0434 respectively. Based on Eq. (14) and data listed in Table III, the grey relational grades were calculated by using these weights of corresponding performance parameter and grey relational coefficients after taking sum of these values for each set of experiment, the values of grey relational grades are shown in Table VI. Thus, the optimization design was performed with respect to a single grey relational grade rather than complicated performance characteristics. According to performed experiment design, it is clearly observed from Table VI that the HS-EDMM parameters setting of experiment No. (18) has the highest grey relational grade. Thus, the eighteenth experiment gives the best multi performance characteristics among the eighteen experiments.

The response table was employed to calculate the average grey relational grade for each HS-EDMM parameter

level. It was done by sorting out the grey relational grades corresponding to levels of the HS-EDMM parameter in each column of the orthogonal ay, and taking an average on those with the same level. Using the same method, calculations were performed for each HS-EDMM parameter level and the response table was constructed as shown in Table (7). Basically, the larger the grey relational grade, the better are the multiple-performance characteristics. In Table (5), A_6 and B_2 show the largest value of grey relational grade for factors A and B. Therefore, A_6B_2 is the condition for the optimal parameter combination of the HS-EDMM.

TABLE VI GREY RELATIONAL GRADE AND ITS ORDER

Exp. No.	Grey relational grade	Order
1	0.6497	4
2	0.6470	5
3	0.5730	16
4	0.6520	3
5	0.6234	8
6	0.5436	18
7	0.6363	7
8	0.5957	12
9	0.5954	13
10	0.5940	14
11	0.6120	9
12	0.5895	15
13	0.6053	10
14	0.6580	2
15	0.6039	11
16	0.5700	17
17	0.6431	6
18	0.6640	1

TABLE VII RESPONSE TABLE FOR THE GREY RELATIONAL GRADE

HD-EDMM Parameters →	Voltage (A)	Capacitance (B)
Level ↓		
1	0.6233	0.6179
2	0.6063	0.6299*
3	0.6091	0.5949
4	0.5985	
5	0.6224	
6	0.6257*	
Max-Min	0.0272	0.0350

-*Optimum

When the last column of performance parameters in Table VII is compared with each other, it is observed that the difference between the maximum and minimum value of the grey relational grade for factor B is the more than factors A. This indicates that the capacitance of capacitors has stronger effect on the multi-performance characteristics followed by gap voltage.

V. CONCLUSIONS

HS-MEDM of 0.5mm thick sheet of Ti-6Al-4V has been carried out and grey relational analysis coupled with principal component analysis optimization strategy has been used to determine the optimal combination of control parameters. The results of the present study are summarized as:

- The responses obtained from the Taguchi method can convert optimization of the multiple-performance characteristics into optimization of a single performance characteristic called the grey relational grade. As a result, optimization of complicated multiple - performance characteristics can be greatly simplified through this approach.
- The principal component analysis which is used to determine the corresponding weighting values of each performance characteristics while applying grey relational analysis to a problem with multiple-performance characteristics is proven to be capable of objectively reflecting the relative importance for each performance characteristic.
- The optimal combination of the HS-EDMM parameters obtained from the proposed method is the set with gap voltage 140V and 100nF capacitance of capacitor.

REFERENCES

- [1] V.K. Jain, 2010, Introduction to Micromachining, Narosa Publishing House, India.
- [2] Y. S. Wong, M. Rahman, H. S. Lim, H. Han, N. Ravi, 'Investigation of micro-EDM material removal characteristics using single RC-pulse discharges', *Journal of Material Processing Technology*, 2003, Vol. 140, pp. 303-307.
- [3] Z.C. Lin and C. Y. Ho, 'Analysis and application of grey relation and ANOVA in chemical-mechanical polishing process parameters', *International Journal of Advanced Manufacturing Technology*, 2003, Vol. 4, pp. 10-14.
- [4] Z. Wansheng, Z. W. Yang, Z. Yong, 'A CAD/CAM system for micro-ED-milling of small 3D freeform cavity', *Journal of Materials Processing Technology*, 2004, Vol. 149, pp. 573-578.

- [5] I. Yoshihito, N. Takayuki, M. Hidetaka, H. Hirofumi, T. Hitoshi, 'Local actuator module for highly accurate micro-EDM', *Journal of Materials Processing Technology*, 2003, Vol. 149, pp. 328-333.
- [6] T. Hideki, H. Hiroaki, M. Naotake, S. Nagao, 'Development of micro-EDM-center with rapidly sharpened electrode', *Journal of Materials Processing Technology*, 2004, Vol. 149, pp. 112-116.
- [7] H. Fuzhu, W. Shinya, K. Masanori, 'Improvement of machining characteristics of micro-EDM using transistor type isopulse generator and servo feed control', *Precision Engineering*, 2004, Vol. 28, pp. 378-385.
- [8] S. Sona, H. Lim, A.S. Kumar, M. Rahman, M., 'Influences of pulsed power condition on the machining properties in micro EDM', *Journal of Materials Processing Technology*, 2007, Vol. 190, pp. 73-76.
- [9] E. Uhlmann, E., R. Markus, R., 'Investigations on reduction of tool electrode wear in micro-EDM using novel electrode materials', *CIRP Journal of Manufacturing Science and Technology*, 2008, Vol. 1, pp. 92-96.
- [10] M.P. Jahan, Y.S. Wong, M. Rahman, 'A study on the fine-finish die-sinking micro-EDM of tungsten carbide using different electrode materials', *Journal of Materials Processing Technology*, 2009, Vol. 209, pp. 3956-3967.
- [11] S.S. Joshi, S. Dhanik, 'Modeling of a single resistance capacitance pulse discharge in micro-electro discharge machining', *Journal of Manufacturing Science and Engineering*, 2007, Vol. 127, pp. 759-767
- [12] R. Kumar, V. Yadava, 'Finite element thermal analysis of micro-EDM', *International Journal of Nanoparticles*, 2008, Vol. 1, pp. 224-240.
- [13] S. Das, S.S. Joshi, 'Modeling of spark erosion rate in microwire-EDM', *International Journal of Advanced Manufacturing Technology*, 2010, Vol. 48, pp. 581-596.
- [14] Y. Karpat, T. Özel, 'Multi-objective optimization for turning processes using neural network modeling and dynamic-neighborhood particle swarm optimization', *International Journal of Advanced Manufacturing Technology*, 2007, Vol. 35, pp. 234-247.
- [15] N. Tosun, 'Determination of optimum parameters for multi-performance characteristics in drilling by using grey relational analysis', *International Journal of Advanced Manufacturing Technology*, 2006, Vol. 28, pp. 450-455.
- [16] Z. C. Lin, C. Y. Ho, 'Analysis and application of grey relation and ANOVA in chemical-mechanical polishing process parameters', *International Journal of Advanced Manufacturing Technology*, 2003, Vol. 2, pp. 10-14.
- [17] C. L. Chang, C. H. Tsai, L. Chen, 'Applying grey relational analysis to the decathlon evaluation model', *International Journal of Computer Internet Manage*, 2003, Vol. 11, pp 54-62.
- [18] J. L. Deng, 1992, *The essential methods of grey systems*, Wuhan: Huazhong University of Science and Technology Press, China.
- [19] Y. Y. Yang, J. R. Shie, C. H. Huang, 'Optimization of dry machining parameters for high purity graphite in end-milling process', *Material and Manufacturing Processes*, 2006, Vol. 21, pp. 832-837.
- [20] H. Hotelling, 'Analysis of a complex of statistical variables into principal components', *Journal of Education Psychology*, 1933, Vol. 24, pp. 417-441.
- [21] H.C. Fung, P.C. Kang, 'Multi-response optimization in friction properties of PBT composites using Taguchi method and principal component analysis', *Journal of Material Process Technology*, 2005, Vol.170, pp. 602-10.